J. Fluid Mech. (1974), vol. 63, part 4, pp. 641–656
Printed in Great Britain

Numerical and asymptotic solutions for the supersonic flow near the trailing edge of a flat plate at incidence

By P. G. DANIELS
Department of Mathematics, University College, London

(Received 7 August 1973 and in revised form 14 November 1973)

The equations which govern the flow at high Reynolds number in the vicinity of the trailing edge of a finite flat plate at incidence to a uniform supersonic stream are solved numerically using a finite-difference procedure. The critical order of magnitude of the angle of incidence α^* for the occurrence of separation on one side of the plate is $\alpha^* = O(R^{-\frac{1}{4}})$ (Brown & Stewartson 1970), where R is a representative Reynolds number for the flow, and results are computed for three such values of α^* which characterize the possible behaviour of the flow above the plate. The final set of computations leads to a numerical value for the trailing-edge stall angle α_s^*, the angle of incidence which just causes the flow to separate at the trailing edge of the plate. Analytic solutions are available in the form of asymptotic expansions near the trailing edge in terms of the scaled variable of order $R^{-\frac{3}{8}}$. A multi-layer-type of expansion which occurs in the case $\alpha^* = \alpha_s^*$ is presented in detail for comparison with the computed solution.

1. Introduction

The flow near the trailing edge of an aerofoil at incidence to a uniform stream, in the limit as the Reynolds number R tends to infinity, has been studied by Brown & Stewartson (1970) for both compressible and incompressible flows. In the former case they showed that (provided that the necessary assumptions are made regarding the thickness of the aerofoil to exclude the effects of leading-edge stall and of a non-zero trailing-edge angle) for a supersonic mainstream the critical order of magnitude of the angle of incidence α^* for the occurrence of separation at the trailing edge is $\alpha^* = O(R^{-\frac{1}{4}})$; the flow above and below the aerofoil near the trailing edge then has a complicated three-layer or triple-deck structure in which the fundamental problem reduces to that of solving the incompressible boundary-layer equations subject to unconventional boundary conditions. The main aim of this paper is to provide a numerical solution to this problem for three values of the scaled angle of incidence α which characterize the possible flow configurations above the aerofoil.

For the first, α is taken to be small and so the flow is similar to that which occurs at zero incidence, numerical results for which have been presented by the present author (1974). As α is increased, a value is reached at which the Blasius flow above the aerofoil is sustained right to the trailing edge; this angle α_0 is the second for which the flow pattern is computed. Further increase in α eventually results in the occurrence of separation on the upper surface of the foil. The final set of computations leads to a numerical value for the trailing-edge stall angle α_s, the angle of incidence which just causes the flow to separate at the trailing edge.

Because of their parabolic nature, the equations are solved using a numerical marching procedure, which takes special account of the singularity which occurs at the trailing edge. The triple-deck structure provides the second-order terms in the asymptotic expansions of the lift and drag on the aerofoil as $R \to \infty$. The computed values of these terms, which are $O(R^{-\frac{5}{8}})$ and $O(R^{-\frac{7}{8}})$ respectively, are tabulated for each angle of incidence. The computed results are also supplemented by analytic solutions in the form of asymptotic expansions in terms of the scaled variable x of order $R^{-\frac{3}{8}}$; this is possible both as $x \to 0+$ (just downstream of the trailing edge) and as $x \to \infty$. Major emphasis is placed on a multi-layer-type expansion which occurs in the case $\alpha = \alpha_s$ as $x \to 0+$.

2. Formulation of the problem

Given the assumptions referred to in § 1 regarding the thickness of the aerofoil, we may, for simplicity, consider a flat plate of zero thickness in the x^*, y^* plane. The plate is taken to occupy the section $-l \leqslant x^* \leqslant 0$ of the x^* axis with the origin of co-ordinates at the trailing edge. The velocity components in the x^* and y^* direction are u^* and v^* respectively, so that if U_∞ is the supersonic mainstream velocity we have

$$u^* \to U_\infty, \quad v^* \to U_\infty \alpha^* \quad (x^* \to -\infty), \tag{2.1}$$

and according to inviscid theory the slip velocity and pressure on the plate are given by

$$u^* = U_\infty + U_\infty \alpha^* \operatorname{sgn} y^*/(M_\infty^2 - 1)^{\frac{1}{2}}, \tag{2.2}$$

$$p^* = p_\infty - U_\infty^2 \rho_\infty \alpha^* \operatorname{sgn} y^*/(M_\infty^2 - 1)^{\frac{1}{2}}, \tag{2.3}$$

where p^* is the pressure and p_∞, ρ_∞ and M_∞ (> 1) are the pressure, density and Mach number respectively at an infinite distance upstream. Thus Blasius-type boundary layers are formed above and below the plate with external velocities and pressures given by (2.2) and (2.3). These apply except in the regions of discontinuity around the leading and trailing edges.

The triple-deck structure which occurs at the trailing edge is described by Brown & Stewartson (1970). Let R be the Reynolds number of the flow, which is assumed large and is defined by

$$R = U_\infty l/\nu_\infty, \tag{2.4}$$

where ν_∞ is the kinematic viscosity at an infinite distance upstream. For convenience, we also define

$$\epsilon = R^{-\frac{1}{8}}. \tag{2.5}$$

Then, in accordance with Brown & Stewartson we define the non-dimensional variables p_T, x, y, u and v by the following scale transformations in the lower deck above the plate, where $x^* = O(\epsilon^3 l)$ and $y^* = O(\epsilon^5 l)$ $(y^* > 0)$:

$$\frac{p^* - p_\infty}{\rho_\infty U_\infty^2} = \epsilon^2 \frac{C^{\frac{1}{4}} \lambda^{\frac{1}{2}}}{(M_\infty^2 - 1)^{\frac{1}{4}}} p_T(x), \tag{2.6}$$

$$\frac{x^*}{l} = \epsilon^3 \frac{C^{\frac{3}{8}} \lambda^{-\frac{5}{4}}}{(M_\infty^2 - 1)^{\frac{3}{8}}} \left(\frac{T_w}{T_\infty}\right)^{\frac{3}{2}} x, \tag{2.7}$$

$$\frac{y^*}{l} = \epsilon^5 \frac{C^{\frac{5}{8}} \lambda^{-\frac{3}{4}}}{(M_\infty^2 - 1)^{\frac{1}{8}}} \left(\frac{T_w}{T_\infty}\right)^{\frac{3}{2}} y, \tag{2.8}$$

$$\frac{u^*(x^*, y^*)}{U_\infty} = \epsilon \frac{C^{\frac{1}{8}} \lambda^{\frac{1}{4}}}{(M_\infty^2 - 1)^{\frac{1}{8}}} \left(\frac{T_w}{T_\infty}\right)^{\frac{1}{2}} u(x, y), \tag{2.9}$$

$$\frac{v^*(x^*, y^*)}{U_\infty} = \epsilon^3 C^{\frac{3}{8}} \lambda^{\frac{3}{4}} (M_\infty^2 - 1)^{\frac{1}{8}} \left(\frac{T_w}{T_\infty}\right)^{\frac{1}{2}} v(x, y). \tag{2.10}$$

We also define α by the relation

$$\alpha^* = \epsilon^2 C^{\frac{1}{4}} \lambda^{\frac{1}{2}} (M_\infty^2 - 1)^{\frac{1}{4}} \alpha. \tag{2.11}$$

Here T_w is the plate temperature, T_∞ is the temperature at infinity and C is Chapman's constant, which occurs in the linear viscosity law

$$\mu/\mu_\infty = C(T/T_\infty), \tag{2.12}$$

where μ is the coefficient of viscosity. The constant λ arises from the match with the Blasius-type flows upstream of the triple decks and satisfies $\lambda = 2^{-\frac{1}{2}} f''(0)$, where $f''' + ff'' = 0$, $f(0) = f'(0) = 0$ and $f'(\infty) = 1$.

The same transformations are made in the lower deck below the plate $(y^* < 0)$ with $p_T(x)$ replaced by $p_B(x)$, these being the pressure perturbations above and below the plate respectively. The problem then reduces to the following equations in the lower decks:

$$u\frac{\partial u}{\partial x} + v\frac{\partial u}{\partial y} = -\frac{dp}{dx} + \frac{\partial^2 u}{\partial y^2},$$

where
$$p(x) = \begin{cases} p_T(x) & (y > 0), \\ p_B(x) & (y < 0), \end{cases} \tag{2.13}$$

$$\partial u/\partial x + \partial v/\partial y = 0, \tag{2.14}$$

subject to the boundary conditions

$$u \to |y|, \quad p_T \to -\alpha, \quad p_B \to \alpha \quad (x \to -\infty), \tag{2.15}$$

$$u - y \to -A_T(x), \quad \text{where} \quad p_T(x) = +dA_T/dx - \alpha \quad \text{as} \quad y \to +\infty, \tag{2.16}$$

$$u + y \to +A_B(x), \quad \text{where} \quad p_B(x) = -dA_B/dx + \alpha \quad \text{as} \quad y \to -\infty, \tag{2.17}$$

$$u = v = 0 \quad \text{on} \quad y = 0 \quad (x < 0), \tag{2.18}$$

$$p(x) = p_T(x) = p_B(x); \quad u, v \quad \text{smooth for all} \quad y \quad (x > 0). \tag{2.19}$$

Here (2.15) represents the merging with the Blasius-type flows upstream, the limiting values of p_T and p_B following directly from (2.3). Conditions (2.16) and (2.17) follow from the match with the main decks of the triple decks and

(2.18) is the no-slip condition on the plate. Condition (2.19) represents the fact that the two lower decks merge beyond the trailing edge, so that the pressures p_T and p_B must equalize and the flow must be continuous across the wake. As in the symmetric case, the final boundary condition required to obtain a unique solution of the system (2.13)–(2.19) is

$$p \to 0 \quad \text{as} \quad x \to \infty. \tag{2.20}$$

3. Computational procedure

The numerical problem presented by (2.13)–(2.20) is more complicated than that for the symmetric case (Daniels 1974, to be referred to as I) since the flow regions above and below the plate in $x \leqslant 0$ must be considered separately, whilst in $x > 0$ the flow must be treated as a whole. The condition (2.20) plays a passive role, and we have to compute a solution which satisfies (2.13)–(2.19), observe its downstream behaviour and re-compute until (2.20) is satisfied. In this way the parabolic nature of the problem is exploited and the solutions above and below the plate are computed using a step-by-step procedure which marches forward in the x direction.

From the computational viewpoint it is found convenient to eliminate α from the problem posed in $x \leqslant 0, y > 0$ by use of the substitution

$$\overline{p}_T = p_T + \alpha. \tag{3.1}$$

In terms of the variables u, v and $\overline{p}_T$, the system of equations and boundary conditions (2.13)–(2.16) and (2.18) is then exactly that which occurs upstream of the trailing edge for a symmetric plate (I), and in $x \leqslant 0$ is the problem originally posed by Stewartson & Williams (1969) to describe the phenomenon of self-induced separation from an infinite plane wall. As $x \to -\infty$ we have

$$\overline{p}_T \sim A_0 e^{kx} = p_0 e^{k(x-x_T)}, \tag{3.2}$$

where $k = 0{\cdot}8272$, $A_0 = p_0 e^{-kx_T}$ is arbitrary and $\overline{p}_T (x = x_T) = p_0$. Three possible forms of solution exist in $x \leqslant 0$, corresponding to p_0 positive, negative or zero. If $p_0 = 0$ we obtain the trivial solution $\overline{p}_T = 0, u = y, v = 0$, which represents the undisturbed Blasius flow. If $p_0 > 0$, $\overline{p}_T$ continues to increase, the skin friction falls and there is a possibility of separation (Stewartson & Williams 1969), whilst if $p_0 < 0$, $\overline{p}_T$ decreases and the skin friction rises in a manner similar to that in the supersonic flow upstream of a convex corner (Stewartson 1970). In both these latter cases the computed solution is initiated by prescribing the increment p_0, with the velocity profile the uniform shear of (2.15). The solution may then be considered to satisfy (2.15) as $x \to -\infty$ and remains unique to within an origin shift in x, until the value of x_T is known.

Similar remarks apply to the solution in $x \leqslant 0, y < 0$, where we make the substitution

$$\overline{p}_B = p_B - \alpha, \tag{3.3}$$

and the solution is unique once the value of x_B, which fixes the origin of the free interaction solution, is known. In this region the solution is always that for which $p_0 < 0$, since the effect of incidence enhances the favourable pressure gradient caused by the presence of the trailing edge. In the lower deck above the plate, the effect of incidence opposes this favourable gradient and the value of p_0 is negative or positive depending upon whether α is less or greater than α_0. When $\alpha = \alpha_0$ we have $p_0 = 0$ and the Blasius flow above the plate continues right to the trailing edge.

At the trailing edge the boundary conditions are discontinuous and the free interaction solutions referred to above are terminated with the requirement that

$$p_B(0) = p_T(0). \tag{3.4}$$

In $x > 0$ the solution continues in terms of u, v and the unified pressure $p(x)$ and the lower decks are treated as a whole, subject to the boundary conditions (2.16) and (2.17) as $y \to \pm\infty$. Finally we must satisfy condition (2.20), and this, together with (3.4), effectively determines the unknown values of x_T and x_B. In practice, however, to compute the solution for one angle of incidence, it is convenient to solve the semi-inverse problem and fix x_T rather than pre-assign a value to α. The solution for $\bar{p}_T$, u and v is then known in $x \leqslant 0, y > 0$. A suitable value for x_B is then chosen and the solution for $\bar{p}_B$, u and v in $x \leqslant 0$, $y < 0$ is computed. The value of α may now be determined from (3.4) as

$$\alpha = \tfrac{1}{2}(\bar{p}_T(0) - \bar{p}_B(0)), \tag{3.5}$$

and is substituted into the boundary conditions (2.16) and (2.17) to allow the solution to be continued into $x > 0$ from the known profile at $x = 0$. The value of x_B must be chosen so that the final boundary condition (2.20) is satisfied.

In a similar manner to the symmetric case, it was found that if $-x_B$ was too small then the solution became compressive, i.e. the pressure rose in $x > 0$, eventually became positive and terminated in a plateau region, whilst if $-x_B$ was too large the solution was expansive, i.e. the pressure gradient, which was initially adverse in $x > 0$, finally became favourable and the computations ended in a singularity with p tending to $-\infty$. The fundamental solution in which $p \to 0$ as $x \to \infty$ clearly divided those results which were compressive from those which were expansive and thus it was possible to compute a solution downstream and adjust x_B accordingly. In this way x_B (and α) were made to converge to values sufficiently accurate to ensure that a compressive and expansive solution were identical, to within a required tolerance, as far downstream as was required and the fundamental solution satisfying (2.20) was thus determined.

The numerical scheme followed a similar pattern to that employed for the symmetric plate (I), the major difference being that now the entire flow field (both $y < 0$ and $y > 0$) had to be considered; in $x \leqslant 0$ and $x > 1$ the equations were discretized onto a mesh of uniform steps in x and y, whilst in $0 < x \leqslant 1$ a double-region matching procedure, an extension of that refined by Smith (1974), was used to enable the solution to pass through the singularity at $x = 0$ in a stable manner (the changeover point $x = 1$ being chosen for convenience). This involved a discretization of the equations into an inner mesh of uniform steps in $\xi\ (\equiv x^{\frac{1}{3}})$ and $\eta\ (\equiv y/x^{\frac{1}{3}})$, enclosed above and below by outer meshes of uniform steps in ξ and y; the numerical scheme thus closely followed the analytical structure of the solution just downstream of the trailing edge, which is outlined in §5.

4. Numerical results

The computations were carried out for three values of α, corresponding to p_0 less than, equal to and greater than zero for the free interaction solution above the plate. For the last of these, x_T was chosen to cause the flow to separate precisely at the trailing edge of the plate and the computations thus yielded the trailing-edge stall angle as $\alpha_s = 2{\cdot}050$, which, if we assume Chapman's constant to be unity, corresponds to an angle of approximately 5° at a Mach number of 2 and Reynolds number of 10^5. For this angle, steps of 0·1 in $x\,(x \leqslant 0,\ x > 1)$ and 0·2 in y were used, with steps of 0·02 in ξ and 0·2 in η in the double region $0 < x \leqslant 1$, whilst for the other two solutions, in which the lower decks remained comparatively thin, the y and η step lengths were halved. In the double region, the outer boundaries of the inner region were taken at $\eta_{\pm\infty} = \pm 5$, which allowed a simple continuation between the double- and single-region schemes at $x = 1$. The outer boundaries for y were chosen to allow the value of $|\partial u/\partial y|$ to tend smoothly to unity and typical values ranged from $y_{\pm\infty} \simeq \pm 6$, for the smallest value of α, to $y_\infty = 15$, and $y_{-\infty} = -1$, for large values of x in the deflected wake downstream of the trailing edge in the case $\alpha = \alpha_s$. All iterations were required to converge to within a tolerance of 10^{-7}. Truncation errors due to the termination of the Taylor series expansions of p, u etc., are thought to be the most likely cause of inaccuracy and as in the symmetric case, the error margin is thought to be of order 5×10^{-4}. Details of the final compressive and expansive solutions computed for each of the three values of α are shown in table 1, where $\tau(x, 0\pm) = \partial u(x, 0\pm)/\partial y$ is the non-dimensional skin friction above and below the plate.

The triple-deck structure at the trailing edge provides the leading-order corrections to the lift and drag due to the boundary-layer flow over the remainder of the plate. In terms of the non-dimensional variables these corrections are

$$L_1 = \epsilon^5 \frac{\rho_\infty l U_\infty^2 C^{\frac{5}{8}}}{\lambda^{\frac{3}{4}}(M_\infty^2 - 1)^{\frac{5}{8}}} \left(\frac{T_w}{T_\infty}\right)^{\frac{3}{2}} I_1, \tag{4.1}$$

$$D_1 = \epsilon^7 \frac{\rho_\infty l U_\infty^2 C^{\frac{7}{8}}}{\lambda^{\frac{1}{4}}(M_\infty^2 - 1)^{\frac{3}{8}}} \left(\frac{T_w}{T_\infty}\right)^{\frac{3}{2}} I_2, \tag{4.2}$$

respectively, where

$$I_1 = -\int_{-\infty}^{0} \bar{p}_T(x)\,dx + \int_{-\infty}^{0} \bar{p}_B(x)\,dx, \tag{4.3}$$

$$I_2 = \int_{-\infty}^{0} \left\{\frac{\partial u}{\partial y}(x, 0+) - 1\right\} dx - \int_{-\infty}^{0} \left\{\frac{\partial u}{\partial y}(x, 0-) + 1\right\} dx. \tag{4.4}$$

On substitution of the numerical value of the constant $\lambda = 0{\cdot}3321$, the coefficients of the total lift L and drag D for the inclined plate may be written as

$$C_L = \frac{L}{\rho_\infty l U_\infty^2} \sim \frac{1{\cdot}152\alpha}{R^{\frac{1}{4}}} \left(\frac{C^{\frac{1}{4}}}{(M_\infty^2 - 1)^{\frac{1}{4}}}\right) + \frac{I_1}{R^{\frac{5}{8}}} \left(\frac{C^{\frac{5}{8}}}{\lambda^{\frac{3}{4}}(M_\infty^2 - 1)^{\frac{5}{8}}} \left(\frac{T_w}{T_\infty}\right)^{\frac{3}{2}}\right) \quad \text{as} \quad R \to \infty, \tag{4.5}$$

$$C_D = \frac{D}{\rho_\infty l U_\infty^2} \sim \frac{1{\cdot}328}{R^{\frac{1}{2}}} C^{\frac{1}{2}} + \frac{I_2}{R^{\frac{7}{8}}} \left(\frac{C^{\frac{7}{8}}}{\lambda^{\frac{1}{4}}(M_\infty^2 - 1)^{\frac{3}{8}}} \left(\frac{T_w}{T_\infty}\right)^{\frac{3}{2}}\right) \quad \text{as} \quad R \to \infty. \tag{4.6}$$

	Solution 1	Solution 2	Solution 3
x_T	−15·7000	—	−18·5075
$p_0 = \bar{p}_T(x_T)$	−0·000001	0	0·000001
Compressive			
x_B	−16·28975	−16·62102	−17·07881
α	0·21170	0·67902	2·05019
$p(0)$	−0·64234	−0·67902	−1·02559
$\tau(0-, 0+)$	1·55371	1·0	0·00000
$\tau(0-, 0-)$	−2·14233	−2·88566	−5·47250
Expansive			
x_B	−16·28978	−16·62104	−17·07882
α	0·21172	0·67904	2·05021
$p(0)$	−0·64236	−0·67904	−1·02561
$\tau(0-, 0+)$	1·55371	1·0	0·00000
$\tau(0-, 0-)$	−2·14238	−2·88572	−5·47257

TABLE 1

α	$I_1/\lambda^{\frac{3}{4}}$	$I_2/\lambda^{\frac{1}{4}}$
0·0	0.0	2·026
0·2117	−0·741	2·012
0·6790	−2·738	1·902
2·0502	−9·539	1·106

TABLE 2

The numerical values of $I_1/\lambda^{\frac{3}{4}}$ and $I_2/\lambda^{\frac{1}{4}}$, including the case $\alpha = 0$ taken from I, are shown in table 2.

Figures 1 and 2 show the general properties of the three solutions computed, and the curves corresponding to $\alpha = 0$ are included for comparison. The solutions are extrapolated for large $x > 0$ using the known asymptotic solution as $x \to \infty$ which is outlined in §6.

5. Asymptotic structure as $x \to 0+$

This region of the flow is important as both the pressure and velocity variations are large compared with those upstream and downstream of the trailing edge in the lower deck, and the expansions, outlined below, indicate the appropriate procedure for the numerical solution in $0 < x \leqslant 1$. At $x = 0-$ we assume that the velocity profile is differentiable and may be written as

$$u(0-, y) = u_0(y), \tag{5.1}$$

where

$$u_0(y) = \begin{cases} a_1 y + a_2 y^2 + a_4 y^4 + \dots & \text{when} \quad |y| \ll 1 \quad (y > 0), & (5.2) \\ b_1 y + b_2 y^2 + b_4 y^4 + \dots & \text{when} \quad |y| \ll 1 \quad (y < 0), & (5.3) \end{cases}$$

and where a_n and b_n $(n = 1, 2, \dots)$ are known constants for a given value of α.

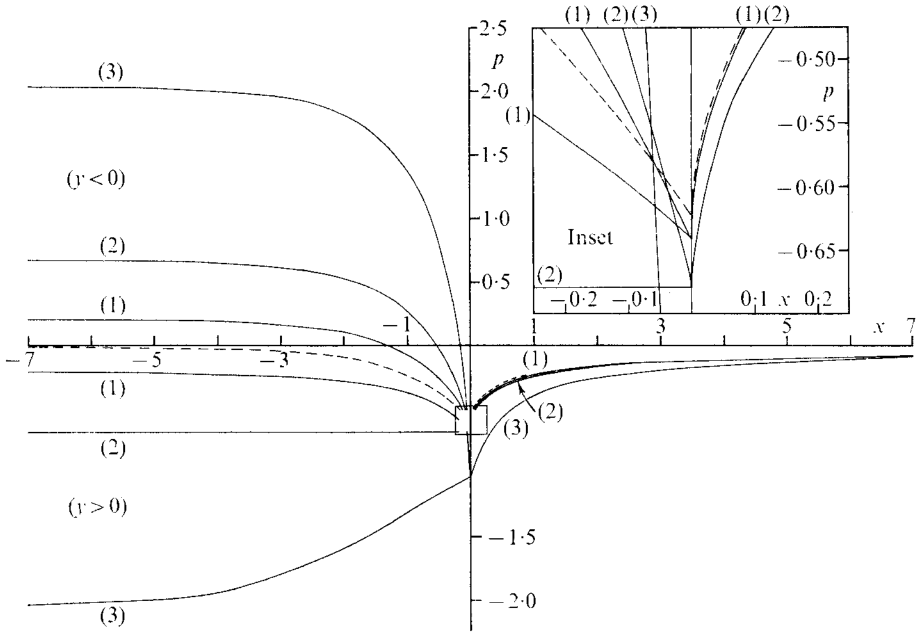

FIGURE 1. The pressure distribution for each angle of incidence: (1) $\alpha = 0{\cdot}2117$, (2) $\alpha = 0{\cdot}6790$, (3) $\alpha = 2{\cdot}0502$. The broken curve corresponds to $\alpha = 0$ and is included for comparison. The behaviour near $x = 0$ is shown in the inset.

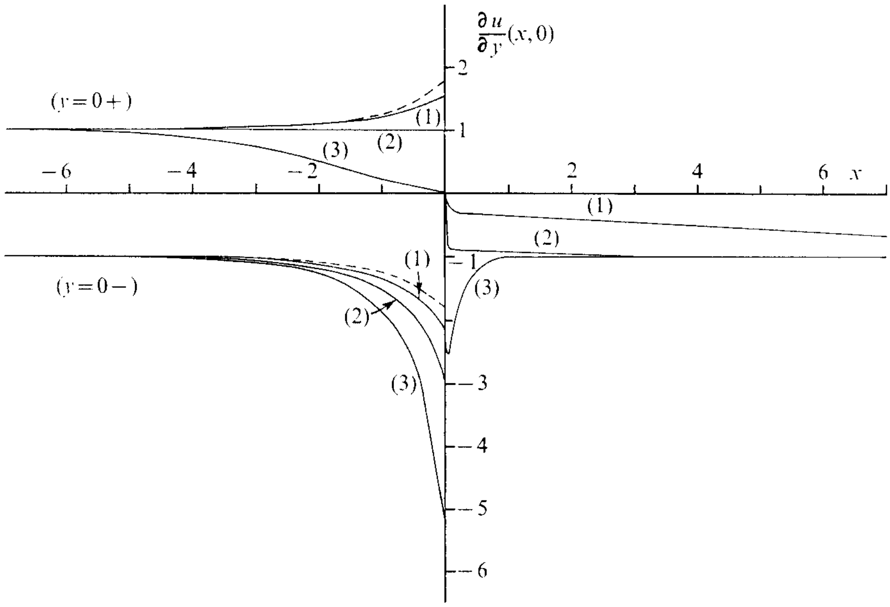

FIGURE 2. The skin friction above and below the plate ($x \leqslant 0$) and the value of $\partial u(x,0)/\partial y$ ($x > 0$) for each angle of incidence: (1) $\alpha = 0{\cdot}2117$, (2) $\alpha = 0{\cdot}6790$, (3) $\alpha = 2{\cdot}0502$. The broken curve corresponds to $\alpha = 0$.

In particular, we have $a_1 = \tau(0-, 0+)$ and $b_1 = \tau(0-, 0-) < 0$, as given in table 1. As pointed out by Brown & Stewartson (1970), the case $a_1 = 0$ (i.e. $\alpha = \alpha_s$) needs special attention, and we first consider $a_1 > 0$.

$a_1 > 0$, *no separation*

The leading terms of the asymptotic expansions as $x \to 0+$ are the same as in the incompressible case, and are achieved by a generalization of the Rott & Hakkinen (1965) wake solution, as shown by Brown & Stewartson. Further terms follow in a similar manner to the symmetric case (I).

In the inner region, where $\eta = y/x^{\frac{1}{3}} = O(1)$, as $x \to 0+$

$$\psi(x, y) = x^{\frac{2}{3}} f_0(\eta) + x \log x f_{10}(\eta) + x f_1(\eta) + O(x^{\frac{4}{3}} (\log x)^2). \tag{5.4}$$

Here ψ is the stream function derived from (2.14) and satisfies $\psi(0, 0) = 0$, $u = \partial\psi/\partial y$ and $v = -\partial\psi/\partial x$. The pressure expansion begins

$$p(x) = p(0) + p_1 x^{\frac{2}{3}} + p_{10} x \log x + p_2 x + O(x^{\frac{4}{3}} (\log x)^2). \tag{5.5}$$

In the outer regions $y < 0$ and $y > 0$, where $y = O(1)$, as $x \to 0+$

$$\psi(x, y) = \psi_0(y) + (x^{\frac{2}{3}} p_1 + x \log x\, p_{10})\, u_0(y) \int_y^i \frac{dy_1}{[u_0(y_1)]^2} + x\psi_2(y) + O(x^{\frac{4}{3}} (\log x)^2). \tag{5.6}$$

Here $\quad \psi_0'(y) = u_0(y), \quad \psi_2(y) = u_0(y) \left\{ \int_y^i \frac{p_2 - u_0''(y_1)}{[u_0(y_1)]^2}\, dy_1 - p(0) - \alpha \operatorname{sgn} y \right\}, \quad (5.7)$

and $i = \pm\infty$ ($y \gtrless 0$). The functions f_0, f_{10} and f_1 and the constants p_1, p_{10} and p_2 satisfy the same equations as in the symmetric case, but now extended to the range $-\infty < \eta < \infty$ and with the boundary conditions modified accordingly. The leading terms satisfy

$$f_0''' + \tfrac{2}{3} f_0 f_0'' - \tfrac{1}{3} f_0'^2 = \tfrac{2}{3} p_1, \quad f_0' - a_1 \eta \to 0 \quad (\eta \to \infty), \quad f_0' - b_1 \eta \to 0 \quad (\eta \to -\infty), \tag{5.8}$$

solutions for which are given by Brown & Stewartson (1970) for a range of the positive parameter $-a_1/b_1$.

$a_1 = 0$, *separation at the trailing edge*

The above theory applies until separation just occurs above the plate at the trailing edge, in which case $a_1 = 0$. According to the computations, this is when $\alpha = \alpha_s = 2{\cdot}050$ and the velocity profile at $x = 0-$ has the properties

$$a_1 = 0, \quad a_2 = \tfrac{1}{2} dp_T(0-)/dx = 0{\cdot}133, \quad b_1 = \tau(0-, 0-) = -5{\cdot}473. \tag{5.9}$$

We find that in this case the three-layer structure which holds for $a_1 > 0$ has to be modified by the insertion of a fourth layer in $y > 0$, where $y = O(x^{\frac{2}{9}})$, and in each layer the expansions proceed in powers of $x^{\frac{1}{9}}$ until the intervention of logarithmic terms. The reason for this format might at first sight seem somewhat arbitrary, but the necessity for a fourth layer becomes immediately obvious if we attempt an expansion of the type used for $a_1 > 0$; suppose that we assume the leading terms to be of the same form as those given by (5.4)–(5.6). Since $a_1 = 0$ we shall have $f_0' \to 0$ as $\eta \to \infty$, and (5.8) is thus only compatible if $p_1 = 0$. Also, since $b_1 < 0$, the solution of (5.8) has $f_0 \to C_0 > 0$ $(\eta \to \infty)$, where C_0 is a constant (see, for example, Stewartson & Williams 1973), and this contributes a term $C_0 x^{\frac{2}{3}}$ to ψ as $\eta \to \infty$. However, since $p_1 = 0$, the equation for the second-order term $x^{\frac{2}{3}}\psi_1(y)$ in the outer region $(y > 0)$ becomes

$$\psi_0 \psi_1' - \psi_0'' \psi_1 = 0, \tag{5.10}$$

with solution $\psi_1 = B\psi_0'$, where B is a constant. From (2.16) we see that $\psi_0'' \to 1$ as $y \to \infty$, so that in order for $\psi_1'(y)$ to satisfy the required boundary condition we must have $B = 0$. But this implies $C_0 = 0$, which is a contradiction.

The reason why the asymptotic structure which holds for $a_1 > 0$ cannot be carried over to the case $a_1 = 0$ is the existence of a small region of slowly moving fluid just downstream of the trailing edge with $0 < y \ll 1$. This region, which, as we shall see, consists of a small bubble of reversed flow, occurs as a result of the adverse pressure gradient above the plate. Whilst the fluid immediately downstream of the trailing edge on $y = 0$ responds to the change in boundary condition by immediately accelerating to a positive velocity, the transmission of the effect of the change in boundary condition to the fluid in the overlying region is not fast enough to prevent the decelerating flow above the plate from attaining a negative velocity just downstream of the trailing edge for $0 < y \ll 1$. In this slowly moving region of reversed flow viscous effects are relatively unimportant and the inertia terms must be balanced by the pressure gradient, which is consequently weaker $(O(x^{-\frac{1}{9}}))$ than in the case of no separation, where it was $O(x^{-\frac{1}{3}})$. It is viscous effects, however, which dominate the flow which spans the region $y = 0-$ to $y = 0+$ just behind the trailing edge, for here the shear $\partial u/\partial y$ must be increased from $b_1 (< 0)$ at $y = 0-$ to zero at $y = 0+$. The combined effect of this shear layer and the shear flow above the plate where $y = O(1)$ (which satisfies $\partial u/\partial y \to 1$ as $y \to \infty$) accelerates the stagnant fluid in the small reversed-flow bubble in between.

The problem now is to provide a precise analytical representation of the physical situation described in the previous paragraph, and we find that the structure of the solution as $x \to 0+$ consists in part of an inner layer surrounding the x axis where $\eta = O(1)$, which is governed by third-order ordinary differential equations and which corresponds to the region of high shear behind the trailing edge. This extends upwards into a transitional layer, which corresponds to the region of slowly moving fluid, where $\theta = y/x^{\frac{2}{9}} = O(1)$ and the governing equations are second order. This region itself extends upwards into an outer layer where $y = O(1)$ and the governing equations are first order. The inner layer extends downwards into a similar outer layer in $y < 0$.

We consider first the outer layers in $y < 0$ and $y > 0$, where, as in the case $a_1 > 0$, successive terms are forced by the pressure expansion, which begins

$$p(x) = p(0) + x^{\frac{8}{9}} P_1 + \dots \quad (x \to 0+). \tag{5.11}$$

Here the appearance of terms of order $x^{\frac{2}{3}}$ or $x^{\frac{7}{9}}$ might be expected, but these may formally be shown to be zero to obtain a consistent solution in the inner regions. The unknown constant P_1 forces the leading-order perturbation $\Phi_1(y)$ of the basic solution $\Phi_0(y)$ in the outer layers so that in both these regions the stream function has the form

$$\psi(x,y) = \Phi_0(y) + x^{\frac{8}{9}}\Phi_1(y) + \dots \quad (x \to 0+), \tag{5.12}$$

where
$$\Phi_0'(y) = u_0(y) \sim -y + A_B(0) \quad (y \to -\infty),$$
$$\Phi_0'(y) \sim y - A_T(0) \quad (y \to \infty) \quad \text{and} \quad \Phi_0'\Phi_1' - \Phi_0''\Phi_1 = -P_1.$$

The boundary conditions (2.16) and (2.17) require that $\Phi_1' \to 0$ ($|y| \to \infty$), so that the appropriate solution is

$$\Phi_1(y) = P_1 u_0(y) \int_y^i \frac{dy_1}{[u_0(y_1)]^2}, \tag{5.13}$$

and as $y \to 0-$ we have

$$\psi(x,y) \sim [\tfrac{1}{2}b_1 y^2 + \tfrac{1}{3}b_2 y^3 + \dots] + x^{\frac{8}{9}}[P_1/b_1 + \dots] + \dots, \tag{5.14}$$

while as $y \to 0+$

$$\psi(x,y) \sim [\tfrac{1}{3}a_2 y^3 + \dots] + x^{\frac{8}{9}}[P_1/3a_2 y + \dots] + \dots. \tag{5.15}$$

In the inner region, where $\eta = y/x^{\frac{1}{3}} = O(1)$, we write the stream function to leading order as

$$\psi(x,y) = x^{\frac{2}{3}}F_0(\eta) + \dots \quad (x \to 0+), \tag{5.16}$$

as in the case $a_1 > 0$. Here the inertia terms are balanced by the viscous term and F_0 satisfies the equation

$$F_0''' + \tfrac{2}{3}F_0F_0'' - \tfrac{1}{3}F_0'^2 = 0. \tag{5.17}$$

The boundary conditions on F_0 as $\eta \to -\infty$ follow from the match with the outer solution in $y < 0$ and we rewrite (5.14) in terms of x and η to obtain

$$\psi(x,y) = x^{\frac{2}{3}}(\tfrac{1}{2}b_1\eta^2) + O(x^{\frac{8}{9}}) \quad (x \to 0+), \tag{5.18}$$

so that F_0 must satisfy the *two* conditions

$$F_0 - \tfrac{1}{2}b_1\eta^2 \to 0 \quad (\eta \to -\infty). \tag{5.19}$$

The third boundary condition needed to complete the solution of (5.17) must come from a condition on F_0 as $\eta \to \infty$. However, if we rearrange the expression (5.15) in terms of x and η we see that there is no term $O(x^{\frac{2}{3}})$ in the resulting expansion, which would imply that $F_0 \to 0$ as $\eta \to \infty$. However, (5.17), with boundary conditions (5.19), has no such solution.

Because of the impossibility of a match between the inner and outer layers in $y > 0$ we postulate the existence of a transitional layer between the two in which the similarity variable is $\theta = y/x^{\frac{2}{9}}$. If we rewrite (5.15) in terms of x and θ we have

$$\psi(x,y) = x^{\frac{2}{3}}(\tfrac{1}{3}a_2\theta^3 + (P_1/3a_2\theta) + \dots) + O(x^{\frac{7}{9}}) \quad (x \to 0+), \tag{5.20}$$

so that in the transitional region we write the stream function to leading order as

$$\psi(x,y) = x^{\frac{2}{3}}G_0(\theta) + \dots \quad (x \to 0+). \tag{5.21}$$

Here then the streamwise velocity u is $O(x^{\frac{4}{9}})$ and the fluid is thus slow-moving in comparison with the viscous flow in the inner region, where $u = O(x^{\frac{1}{3}})$, and with the outer flow above. The inertia terms are balanced by the pressure gradient and we have

$$G_0 G_0''' - \tfrac{2}{3} G_0'^2 = \tfrac{4}{3} P_1, \tag{5.22}$$

where, from (5.20), G_0 must satisfy

$$G_0 \sim \tfrac{1}{3} a_2 \theta^3 + (P_1/3a_2\theta) \quad (\theta \to \infty). \tag{5.23}$$

At $\theta = 0$ we have

$$G_0(\theta) = c_1 + c_2\theta + [(c_2 + 2P_1)/3c_1]\,\theta^2 + \ldots, \tag{5.24}$$

where c_1 and c_2 are arbitrary constants ($c_1 \neq 0$), and if we rewrite (5.21) in terms of x and η as $\theta \to 0$ we find that we require

$$\psi(x, y) \sim x^{\frac{2}{3}} c_1 + O(x^{\frac{7}{9}}), \tag{5.25}$$

as $\eta \to \infty$. Thus the appropriate boundary condition on F_0 as $\eta \to \infty$ is in fact

$$F_0' \to 0 \quad (\eta \to \infty), \tag{5.26}$$

and the solution of (5.17) determines c_1 as $c_1 = C_0$, where C_0 is the constant mentioned earlier. The leading-order equation (5.22) in the transitional region may then be solved for G_0 and P_1 subject to the three conditions $G_0(0) = c_1$ (from (5.24)) and $G_0 \sim \frac{1}{3} a_2 \theta^3 + 0 \times \theta^2$ $(\theta \to \infty)$ (from (5.23)); knowledge of the constant P_1 completes the leading-order solutions (5.13) in the outer regions.

Further terms in the expansions of p and ψ in each region follow in powers of $x^{\frac{1}{9}}$ until logarithms occur for a similar reason to that causing logarithms to arise in the case $a_1 > 0$, a full explanation of which is given in I for the case $\alpha = 0$. The formal expansions as $x \to 0+$ are

$$p = p(0) + \sum_{n=1}^{5} P_n x^{\frac{1}{9}(n+7)} + P_{60} x^{\frac{13}{9}} \log x + O(x^{\frac{13}{9}}), \tag{5.27}$$

with

$$\psi = \Phi_0(y) + \sum_{n=1}^{5} \Phi_n(y)\, x^{\frac{1}{9}(n+7)} + \Phi_{60} x^{\frac{13}{9}} \log x + O(x^{\frac{13}{9}}) \tag{5.28}$$

in the outer regions,

$$\psi = \sum_{n=0}^{4} x^{\frac{1}{9}(n+6)} F_n(\eta) + F_{50}(\eta)\, x^{\frac{11}{9}} \log x + O(x^{\frac{11}{9}}) \tag{5.29}$$

in the inner region and

$$\psi = \sum_{n=0}^{4} x^{\frac{1}{9}(n+6)} G_n(\theta) + G_{50}(\theta)\, x^{\frac{11}{9}} \log x + O(x^{\frac{11}{9}}) \tag{5.30}$$

in the transitional region.

The equations for F_n and G_n $(n = 0, 1, \ldots)$ must be solved alternately; at each stage the solution F_n produces the appropriate condition at $\theta = 0$ to obtain the solution for G_n and P_{n+1} and hence complete the solution in each region. The solution G_n in turn determines the boundary condition at $\eta = \infty$ for the solution for F_{n+1} and so on. The first four equations in the inner and transitional regions were solved numerically using a program kindly loaned by Mr P. G. Williams; F_0, G_0 and P_1 were first found in the manner already described and the constant c_2 is thus determined as $c_2 = G_0'(0)$. The function F_1 is then found as the solution of the equation

$$F_1'''' + \tfrac{2}{3} F_0 F_1''' - \tfrac{7}{9} F_0' F_1' + \tfrac{7}{9} F_0'' F_1 = 0, \tag{5.31}$$

x	p_c	p_A
0·0	−1·02560	−1·02560
0·000008	−1·02558	−1·02558
0·000064	−1·02545	−1·02546
0·000216	−1·02511	−1·02516
0·000512	−1·02450	−1·02463
0·001	−1·02355	−1·02377

TABLE 3

subject to the boundary conditions

$$F_1' \to c_2 \quad (\eta \to \infty), \quad F_1 \sim 0 \times \eta^{\frac{7}{3}} + 0 \times \eta + O(e^{-\frac{1}{9}b_1\eta^3}/\eta^4) \quad (\eta \to -\infty). \tag{5.32}$$

Here the condition as $\eta \to \infty$ follows from the match with the inner limit (5.24) in the transitional region, whilst the two conditions as $\eta \to -\infty$ follow from (5.18). The equation for G_1 is

$$\tfrac{2}{3}G_0 G_1'' - G_0' G_1' + \tfrac{7}{9}G_0'' G_1 = P_2 - G_0''', \tag{5.33}$$

and the boundary conditions provided by the match with the inner region as $\theta \to 0$ and with the outer layer as $\theta \to \infty$ are

$$G_1(0) = c_3 = \lim_{\eta \to \infty} \{F_1(\eta) - c_2\eta\}, \quad G_1(\theta) \sim 0 \times \theta^{\frac{7}{2}} + 0 \times \theta^2 \quad (\theta \to \infty). \tag{5.34}$$

The unknown parameter P_2 is thus determined and completes the solution for Φ_2 in the outer layers, which is the same as the solution for ψ_2 given by the expression (5.7) with p_2 replaced by P_2.

The numerical results were

$$P_1 = 0{\cdot}599, \quad P_2 = 0{\cdot}521, \tag{5.35}$$

$$c_1 = 2{\cdot}206, \quad c_2 = -1{\cdot}426, \quad c_3 = 1{\cdot}829, \tag{5.36}$$

with the following velocity profile at $y = 0$:

$$u(x,0) \sim 1{\cdot}893x^{\frac{1}{3}} - 0{\cdot}211x^{\frac{4}{9}} + O(x^{\frac{5}{9}}). \tag{5.37}$$

In the matching zone ($\eta = \infty$, $\theta = 0$) the reversed-flow region is in evidence and we have

$$u(x,y) \sim -1{\cdot}426x^{\frac{4}{9}} - 1{\cdot}452x^{\frac{5}{9}} + O(x^{\frac{2}{3}}). \tag{5.38}$$

As $\theta \to \infty$ the profile becomes positive again and we have

$$u(x,y) \sim (0{\cdot}133y^2 + \ldots) + O(x^{\frac{8}{9}}). \tag{5.39}$$

This behaviour is demonstrated by the computed profile at $x = 0{\cdot}008$ which is shown in figure 3, and clearly indicates a small region of reversed flow. This was apparently not large enough to cause the failure of the downstream marching procedure and since the computed solution remained stable it was found unnecessary to incorporate the transitional layer in the numerical scheme. With only the first two terms in the asymptotic expansions a quantitative comparison with

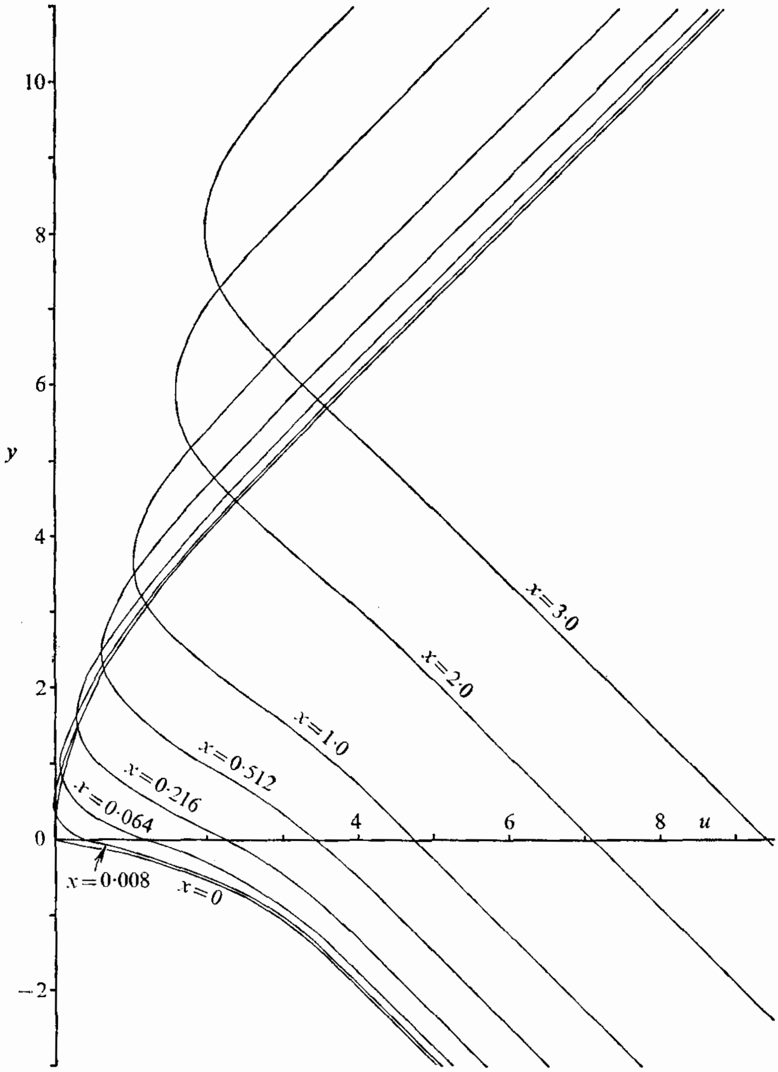

FIGURE 3. Velocity profiles downstream of the trailing edge in the case $\alpha = 2{\cdot}0502$.

the computed solution is only possible for very small values of x, and table 3 shows a comparison between the computed pressure p_c and the asymptotic pressure p_A, calculated from (5.27) using the numerical values (5.35).

6. Asymptotic structure for large x

We first consider the fundamental solution for which $p \to 0$ as $x \to \infty$. The external inviscid flow leaves the trailing edge of the plate parallel to the mainstream, i.e. at an angle α^* to the plate. This must match with the wake formation downstream of the trailing edge in the lower deck and the streamline $\psi = 0$ is given by $y \sim \alpha x$ as $x \to \infty$. In fact we can eliminate α from the boundary conditions (2.16) and (2.17) by applying a transformation of the type used by

Brown & Stewartson (1970) in the incompressible case, which in the supersonic situation is simply
$$\bar{y} = y - \alpha x, \quad \bar{v} = v - \alpha u. \tag{6.1}$$
The resulting equations and boundary conditions in the wake, in terms of the variables $x, \bar{y}, u, \bar{v}$ and p, are then similar to those which occur in the symmetric problem $\alpha = 0$. However, in contrast to that case, here the upstream profiles (at $x = 0$, say) are not symmetric about $\bar{y} = 0$ and the conditions (2.16) and (2.17), which become
$$u - |\bar{y}| \to -\int_0^x p(t)\,dt - \tfrac{1}{2}\{A_T(0) - A_B(0)\} - \tfrac{1}{2}\{A_T(0) + A_B(0)\}\,\mathrm{sgn}\,\bar{y} \quad (|\bar{y}| \to \infty), \tag{6.2}$$
may not be replaced in part by the symmetry condition $\bar{v} = \partial u/\partial \bar{y} = 0$ at $\bar{y} = 0$. Asymmetries thus occur in the expansions for large x, and take the form of arbitrary shifts in the origin of $\bar{\eta}$, which is defined as the similarity variable $\bar{y}/x^{\frac{1}{3}}$.

We expect the expansions which satisfy condition (2.20) to be of the form
$$p(x) \sim \bar{p}_0/x^{\frac{2}{3}} + \bar{p}_1/x^{\frac{4}{3}} + \ldots \quad (x \to \infty), \tag{6.3}$$
with
$$\psi(x, y) \sim x^{\frac{2}{3}}\bar{f}_0(\bar{\eta}) + x^{\frac{1}{3}}\bar{f}_1(\bar{\eta}) + x^{-\frac{1}{3}}\bar{f}_2(\bar{\eta}) + \ldots \quad (x \to \infty). \tag{6.4}$$
The leading terms satisfy
$$\bar{f}_0''' + \tfrac{2}{3}\bar{f}_0\bar{f}_0'' - \tfrac{1}{3}\bar{f}_0'^2 = 0, \quad \bar{f}_0' \sim \bar{\eta} - 3\bar{p}_0 \quad (\bar{\eta} \to \infty), \quad \bar{f}_0' \sim -\bar{\eta} - 3\bar{p}_0 \quad (\bar{\eta} \to -\infty). \tag{6.5}$$
Here we effectively have three boundary conditions, and an origin shift in $\bar{\eta}$ is not possible. The solution is thus determined uniquely, the last condition may be replaced by $\bar{f}_0(0) = \bar{f}_0''(0) = 0$ and we see that $\psi(x, \alpha x) = 0$ to leading order as $x \to \infty$. The numerical solution of (6.5) by Stewartson (1969) in connexion with the symmetric flat plate gives
$$\bar{p}_0 = -0{\cdot}297, \quad \bar{f}_0'(0) = 1{\cdot}611, \tag{6.6}$$
and provides an asymptotic extension to the computed solutions in figure 1.

The first eigenfunction $\bar{f}_1$ is induced by the asymmetric part of the boundary condition (6.2) and satisfies
$$\bar{f}_1' \to -C_1 - \tfrac{1}{2}(A_T(0) - A_B(0)) - \tfrac{1}{2}(A_T(0) + A_B(0))\,\mathrm{sgn}\,\bar{\eta} \quad (|\bar{\eta}| \to \infty), \tag{6.7}$$
where C_1 is the constant in the expansion of
$$\int_0^x p(t)\,dt \quad \text{as} \quad x \to \infty;$$
if $\bar{f}_1(\bar{\eta})$ is any solution which satisfies the two boundary conditions (6.7) then other possible solutions are of the form $\bar{f}_1(\bar{\eta} + c_0)$, where c_0 is an arbitrary constant. The second eigenfunction $\bar{f}_2$ occurs in the symmetric problem and satisfies $\bar{f}_2 \to \frac{3}{2}\bar{p}_1$ as $\bar{\eta} \to \pm\infty$. Here possible solutions are
$$\bar{f}_2(\bar{\eta}) = -(\bar{p}_1/\bar{p}_0)\{\bar{f}_0(\bar{\eta}_0) - \tfrac{1}{2}\bar{\eta}_0\bar{f}_0'(\bar{\eta}_0)\}, \tag{6.8}$$
where $\bar{\eta}_0 = \bar{\eta} + c_{00}$ and c_{00} is an arbitrary constant. $\bar{p}_1$ remains arbitrary, as in the symmetric case, and corresponds to an origin shift in x, whilst c_{00} corresponds to an origin shift in $\bar{\eta}$ and represents a possible asymmetry in the $\bar{y}$ direction.

Finally we mention the compressive and expansive solutions, in which p does not tend to zero as $x \to \infty$. The asymptotic behaviour of these solutions has been fully analysed for the symmetric case and is given in I. For $\alpha \neq 0$ we make the transformation (6.1) and find that, just as for the fundamental solution, the expansions proceed in the same manner as given in I, but in terms of the variables x, $\bar{y}$, u, $\bar{v}$ and p, and with asymmetries which occur in the form of origin shifts in $\bar{y}$. The compressive solutions are the most interesting physically. The pressure approaches a constant positive plateau value as $x \to \infty$ and the boundary layers leaving the trailing edge separate to enclose a region of completely inviscid reversed flow behind the plate, which to leading order is bisected by the line $y = \alpha x$. This may be caused by a small impediment in the flow downstream of the plate. The expansive solutions end with the pressure tending to $-\infty$, and represent a flow which accelerates to a sink-type singularity on the line $y = \alpha x$ at a finite value of x, x_1, say. As shown in I, in this case we have

$$p(x) \sim -2/(x_1 - x)^2 \quad \text{as} \quad x \to x_1 - . \tag{6.9}$$

The author gratefully acknowledges help and encouragement from Dr S. N. Brown, Professor K. Stewartson and Mr P. G. Williams, and the financial support of the S.R.C.

REFERENCES

Brown, S. N. & Stewartson, K. 1970 Trailing-edge stall. *J. Fluid Mech.* **42**, 561–584.

Daniels, P. G. 1974 Numerical and asymptotic solutions for the supersonic flow near the trailing edge of a flat plate. *Quart. J. Mech. Appl. Math.* (in the Press).

Rott, N. & Hakkinen, R. J. 1965 Similar solutions for merging shear flows, II. *A.I.A.A. J.* **8**, 1553–1554.

Smith, F. T. 1974 *J. Inst. Maths. Applics.* (in the Press).

Stewartson, K. 1969 On the flow near the trailing edge of a flat plate, II. *Mathematika*, **16**, 106–21.

Stewartson, K. 1970 On supersonic laminar boundary layers near convex corners. *Proc. Roy. Soc.* A **319**, 289–305.

Stewartson, K. & Williams, P. G. 1969 Self-induced separation. *Proc. Roy. Soc.* A **312**, 181–206.

Stewartson, K. & Williams, P. G. 1973 On self-induced separation, II. *Mathematika*, **20**, 98.